Solid State Ionics 300 (2017) 86–90

Contents lists available at ScienceDirect

Solid State Ionics

journal homepage: www.elsevier.com/locate/ssi

Peculiarities of ionic conduction in $Li_{0.5-y}Na_yLa_{0.5}Nb_2O_6$ system at high temperatures

S. Daugėla [a], A. Kežionis [a], T. Šalkus [a], A.F. Orliukas [a], A.G. Belous [b], O.I. V'yunov [b], S.D. Kobylianska [b], L.O. Vasylechko [c]

[a] Department of Radiophysics, Faculty of Physics, Vilnius University, Saulėtekio ave. 3, LT-10222 Vilnius, Lithuania
[b] Vernadskii Institute of General & Inorganic Chemistry, Palladina ave. 32/34, 03142 Kyiv, Ukraine
[c] Semiconductor Electronics Department, Lviv Polytechnic National University, St. Yura square 1, 79000 Lviv, Ukraine

ARTICLE INFO

Article history:
Received 25 July 2016
Received in revised form 1 December 2016
Accepted 9 December 2016
Available online xxxx

Keywords:
Perovskite
Lithium conductors
Impedance spectroscopy

ABSTRACT

Pure perovskite structure $Li_{0.5-y}Na_yLa_{0.5}Nb_2O_6$ compounds with y values of 0, 0.1, 0.2, 0.3, 0.4, 0.43, 0.48 and 0.5 have been synthesized. Ceramics of these compounds were studied by X-ray diffraction and impedance spectroscopy in the frequency range of 10 Hz to 10 GHz and temperature interval from 300 K to 800 K. The linear increase of the lattice parameters with increasing temperature causes the wider opening of bottleneck for lithium migration which leads to ionic conductivity increase. The temperature dependencies of the studied compounds conductivity were described by modified Vogel–Fulcher–Tammann equation. The influence of Li^+ to Na^+ substitution to the lithium ionic transport is also analysed. On one hand the lattice parameters of $Li_{0.5-y}Na_yLa_{0.5}Nb_2O_6$ were found to be bigger for compound with higher sodium concentration, which also increases their ionic conductivity. On the other hand the increase of y leads to decrease of charge carriers, which are lithium ions, concentration. Consequently the conductivity rapidly decreases.

1. Introduction

The oxide-based lithium-ion conductors deserve much attention because of their possible applications as solid electrolytes or electrode materials in various electrochemical devices such as batteries, sensors, supercapacitors and electrochromic displays [1–5]. Some of the well know lithium-ion conductors are lithium lanthanum titanate $Li_{3x}La_{2/3-x}\square_{1/3-2x}TiO_3$ (LLTO) and lithium lanthanum niobate $Li_{3x}La_{2/3-x}\square_{4/3-2x}Nb_2O_6$ (LLNbO), both having defected perovskite structure. At room temperature the high ionic conductivity has been reported for these perovskites (10^{-3}–10^{-5} S/cm) [6–8].

In the system $Li_{0.5-x}Na_xLa_{0.5}TiO_3$ (LNLTO) lithium ions are partially substituted by sodium ions, which are not taking part in the conduction process due to ionic radii difference. So sodium ions block lithium conduction pathways by sharing the same crystallographic sites. In the case of LNLTO percolation model has been successfully applied to describe ionic conductivity [9–11]. The investigation results on LLTO system have shown that in the temperature interval of 290–400 K mobile ion activation energy is 0.3 eV and the conductivity changes according to Arrhenius law [12,13]. However above 400 K non-Arrhenius behaviour of conductivity was observed and Vogel–Fulcher–Tammann (VFT) equation can be used to describe it [14,15]. The data also show that lithium conductivity is affected by number of structural vacancies and also bottleneck sizes of lithium pathways. In order to understand the peculiarities of lithium transport in defected perovskites lithium lanthanum niobate $Li_{3x}La_{2/3-x}\square_{4/3-2x}Nb_2O_6$ was also investigated [16–18]. The investigation of Li → Na substitution in this system showed that the ionic conductivity cannot be described by percolation model, because this system contains significantly higher vacancy concentration in lithium-lanthanum sublattice compared to $Li_{3x}La_{2/3-x}\square_{1/3-2x}TiO_3$ [19,20].

It is well known, that the conductivity is a product of mobile lithium-ion concentration ($[Li^+]$), mobile ion charge (e) and their mobility (μ):

$$\sigma_{Li} = [Li^+] \cdot e \cdot \mu. \quad (1)$$

The ionic conductivity in the system $Li_{0.5-y}Na_yLa_{0.5}Nb_2O_6$ at room temperature shows a maximum ~1.3×10^{-5} S/m for y = 0.43 [18,19]. Knowing, that sodium ions do not participate in the conduction process, authors [19] explain this maximum originating from the increase of perovskite unit cell when lithium is substituted with sodium, and this leads to lithium mobility (μ) increase. However, when y > 0.4 the conductivity σ_{Li} significantly decreases due to decrease of the mobile lithium charge carrier concentration. $Li_{0.5-y}Na_yLa_{0.5}Nb_2O_6$ compounds form superlattice cells and belong to orthorhombic symmetry with space group *Pmmm*. The unit cell parameters and volume of a unit cell increases with the increase of sodium amount in the compound according to Vegard's law [21]. Authors [21] have shown, that La^{3+} ions exceptionally occupy positions in the z = 0 plain of the $Li_{0.5-y}Na_yLa_{0.5}Nb_2O_6$ lattice when 0 ≤ y ≤ 0.3 (see Fig. 1). Consequently 2D conductivity takes place. When the amount of sodium is increased (y > 0.3), La^{3+} cations

http://dx.doi.org/10.1016/j.ssi.2016.12.011
0167-2738/

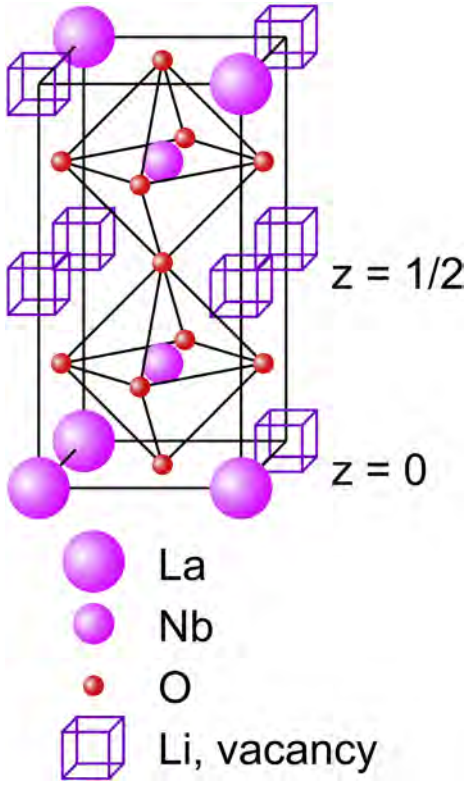

Fig. 1. Crystallographic structure of $Li_{3x}La_{2/3-x}\square_{4/3-2x}Nb_2O_6$.

distribute between z = 0 and 1/2 plains and the transition from 2D to 3D conductivity was observed [18].

The aim of current work is to study the relation of crystal structure with high temperature lithium-ion conductivity in the system $Li_{0.5-y}Na_yLa_{0.5}Nb_2O_6$, because the volume of the crystal lattice can be expanded either by increasing sodium-ion concentration ($r_{Na^+} > r_{Li^+}$), or by increasing temperature. The impedance spectroscopy investigations at high temperatures and in the broad frequency range of these compounds have not been performed before. The investigation of compounds with different lithium-sodium ratio within these perovskites at temperatures up to 800 K allows one to clarify the peculiarities of ionic conductivity.

2. Experimental

The $Li_{0.5-y}Na_yLa_{0.5}Nb_2O_6$ samples with y = 0, 0.1, 0.2, 0.3, 0.4, 0.43, 0.48, and 0.5 were prepared by solid-state reactions. The starting chemicals were La_2O_3 (purity 99.9%, Cerac), extra-pure-grade Nb_2O_5 (99.95%, Cerac), Li_2CO_3 and Na_2CO_3 (99.99%, Aldrich). The synthesis procedure was described in detail earlier [16–18]. The stoichiometric powder mixtures were pressed into pellets, which were fired first at 970 K for 4 h (in order to prevent alkali metal losses during heat treatment) and then at 1320 K for 2 h, with an intermediate grinding. After homogenization by grinding in a vibratory mill with ethanol, followed by drying, an aqueous 5% solution of polyvinyl alcohol was added as a plasticizer. Green compacts (d = 14 mm, p = 80 MPa) were sintered at temperatures from 1470 to 1720 K for 2 h. The current ceramic preparation procedure allowed us to obtain $Li_{0.5-y}Na_yLa_{0.5}Nb_2O_6$ samples with relative density of 95–98%.

The resultant materials were characterized by X-ray diffraction (XRD). XRD patterns were collected on a DRON-4-07 powder diffractometer (CuKα radiation). In order to study the perovskite structure and its thermal evolution in detail in the temperature range from 300 to 1200 K high-resolution powder diffraction experiments have been performed at the experimental station B2 in the synchrotron laboratory HASYLAB (Hamburg, Germany). Structural parameters at various temperatures were determined by the Rietveld full-profile analysis method using XRD data.

The impedance spectroscopy was performed on small cylindrical ceramic samples. Platinum paste was used to prepare electrodes. The length of all samples was 1.5 mm and the electrode surface area was under 1 mm^2. Impedances ($\tilde{Z}$) were measured in the frequency range of 10 Hz to 10 GHz and temperature range from 300 to 800 K with 20 K step. The impedance measurement method is described in detail elsewhere [22]. In order to avoid any affects due to processes on the interface of the Pt electrode and $Li_{0.5-y}Na_yLa_{0.5}Nb_2O_6$ electrolyte additional measurements by four-electrode method were performed [23]. We further use intrinsic materials parameters to describe our ceramics, i.e. complex resistivity ($\tilde{\rho} = \rho' + j\rho'' = \frac{\tilde{Z}l}{S}$, where j is imaginary unit, l is sample length and S – sample electrode area) and complex conductivity ($\tilde{\sigma} = \sigma' + j\sigma'' = \frac{1}{\tilde{\rho}}$). The impedance data were fitted using equivalent circuit models by ZView software.

3. Results

3.1. Crystalline structure

As can be seen from Tables 1 and 2 the lattice parameters and unit cell volume for $Li_{0.5-y}Na_yLa_{0.5}Nb_2O_6$ compounds with y = 0 and 0.5 linearly increase with increasing temperature. Besides the lanthanum site occupancies at z = 0 and z = 1/2 planes do not change in the studied temperature range.

3.2. Ionic conductivity

An example of complex resistivity spectrum for $Li_{0.3}Na_{0.2}La_{0.5}Nb_2O_6$ ceramics is shown in Fig. 2. The figure is a usual resistivity representation in the complex plain and it shows two spectra measured at 300 K by two-electrode method and by four-electrode method.

Two semicircles can clearly be seen from the data obtained by four-electrode method. Such spectrum can easily be modelled by two series processes, each of them were described by resistance (R) connected in parallel with a constant phase element (CPE). The impedance of CPE is expressed as

$$\tilde{Z}_{CPE} = \frac{1}{Q(j\omega)^n}, \quad (2)$$

where $\omega = 2\pi f$ is the angular frequency, and the true capacitance of the process is found from equation

$$C = \frac{(Q \cdot R)^{1/n}}{R}. \quad (3)$$

Table 1
Structure parameters of $Li_{0.5}La_{0.5}Nb_2O_6$ at different temperatures.

T, °C	20	300	600	900
Unit cell parameters				
a, Å	3.899(1)	3.908(1)	3.923(2)	3.931(3)
b, Å	3.901(1)	3.911(1)	3.925(2)	3.933(3)
c, Å	7.8542(6)	7.8791(8)	7.9090(7)	7.9250(6)
V, Å^3	119.48(5)	120.43(5)	121.72(8)	122.5(1)
Site occupancies, La				
z = 0	0.475(4)	0.475(4)	0.472(4)	0.471(4)
z = 1/2	0.065(4)	0.065(4)	0.068(4)	0.069(4)
Agreement factors				
Rp, %	6.23	6.62	7.02	7.09
Rwp, %	7.94	8.39	9.04	9.19

Table 2
Structure parameters of $Na_{0.5}La_{0.5}Nb_2O_6$ at different temperatures.

T, °C	20	300	600	900
Unit cell parameters				
a, Å	3.923(2)	3.936(2)	3.944(1)	3.956(1)
b, Å	3.924(2)	3.935(2)	3.951(1)	3.964(1)
c, Å	7.8512(7)	7.8774(8)	7.9143(5)	7.9368(5)
V, Å^3	120.86(9)	122.01(9)	123.33(4)	124.46(5)
Site occupancies, La				
z = 0	0.256(6)	0.255(8)	0.252(5)	0.257(5)
z = 1/2	0.244(6)	0.245(8)	0.248(5)	0.243(5)
Agreement factors				
Rp, %	7.13	6.73	6.62	6.90
Rwp, %	9.23	8.37	9.15	8.88

The spectrum of each R||CPE connection is of depressed semicircle shape in the complex plain plot. The semicircle at lower frequencies between 10 Hz and 1 kHz can be attributed to ionic relaxation in the grain boundaries of the ceramics with the corresponding typical capacitance value of $1.4 \cdot 10^{-8}$ F. From the diameter of the semicircle the grain boundary conductivity (σ_{gb}) can be found. Similarly, the higher frequency semicircle represents ionic relaxation in the grains (bulk) of ceramics. The grain or bulk conductivity (σ_b) can be found from the diameter of the semicircle and the corresponding capacitance value was $2 \cdot 10^{-12}$ F.

Comparing the spectrum obtained by four-electrode method with the one obtained by two-electrode method, one can see some important differences. The spectrum obtained by two-electrode method has an additional part in the low frequency range (from 12 kHz to 10 Hz), which is attributed to ion blocking at the electrode-electrolyte interface. Therefore the imaginary part of complex resistivity rises with decrease of frequency, which is a clear feature of capacitive electrode nature. The local minimum of ρ'' was found at 12 kHz, which is much higher compared to the four-electrode spectrum (1 kHz). This shows that the grain boundary contribution to the two-electrode spectrum is masked by the processes taking place at the electrode. However, the ionic relaxation frequency in the grains of ceramics (frequency of the grain semicircle maximum) was found to be the same from both measurements, $f = 1/(2\pi RC) = 100$ kHz. So, the grain conductivity σ_b (the diameter of high frequency semicircle) can be found by equivalent circuit modelling from measurements by two-electrode method.

The above analysed example for the composition with y = 0.2 is the most clear. For other compositions similar impedance spectra were obtained, but in some cases only a trace of low frequency semicircle was observed, so precise determination of the grain boundary conductivity was very difficult. In the present work we will focus on analysis of conductivity in the grains of $Li_{0.5-y}Na_yLa_{0.5}Nb_2O_6$ ceramics because of these reasons:

- the conductivity of ceramics grain boundary highly depends on the ceramic quality and microstructure (grain size, density, crack and impurity level, etc.), which may slightly wary among different samples. Only the grain conductivity gives us the information about Li ↔ Na substitution in the system;
- the two-electrode measurement method is much more precise compared to the four-electrode method [23]. As it was shown above, only the grain conductivity can be derived from measurements by two-electrode method;
- as the relaxation frequencies of both processes shift towards higher frequencies with the increase of temperature, the grain conductivity semicircle disappears from four-electrode spectra at higher temperatures due to limited frequency range (up to 2 MHz), while it can be observed by performing two-electrode measurement in the microwave frequency range.

Temperature dependences of lithium-ion conductivity in the ceramic grains with different amount of sodium (y) are presented in Fig. 3. Arrhenius-type conductivity behaviour with temperature was found only for the sample with y = 0. For all other samples the change of activation energy can be observed at high temperatures (>500 K). The lowering of activation energy is observed at higher temperatures for the compounds in which the sodium to lithium substitution ratio is higher (red line in Fig. 3). In the lower temperature range (300–500 K) the activation energy of ~0.4 eV has been found, while at high temperatures it is about 0.2 eV.

Concentration dependences of conductivity in the bulk of ceramics grains obtained from impedance spectroscopy data are presented in Fig. 4. At 300 K the bulk conductivity increases from $1 \cdot 10^{-3}$ to $2.1 \cdot 10^{-3}$ S·m^{-1} when lithium is substituted with sodium and reaches the maximum value at y = ~0.4 (Fig. 4a) and b) curve 1). At 400 K the conductivity increases from $4.8 \cdot 10^{-2}$ to maximal value of $7.2 \cdot 10^{-2}$ S·m^{-1} at about y = 0.3 (Fig. 4b), curve 2). At higher temperatures the conductivity maximum shifts to the direction of lower sodium concentrations, for example at 500 K the maximum value can be found when y = 0.2 (Fig. 4b), curve 3), though at 800 K ionic conductivity lowers continuously with the lithium-ion exchange with sodium (Fig. 4b), curve 4).

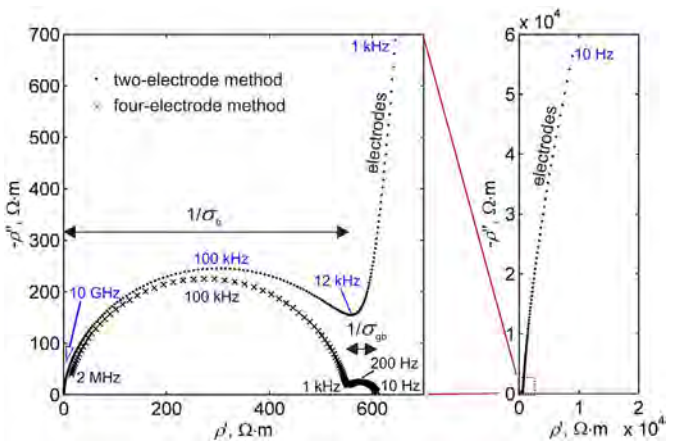

Fig. 2. Complex plain resistivity plots of $Li_{0.3}Na_{0.2}La_{0.5}Nb_2O_6$ ceramics measured at 300 K by two- and four-electrode methods. Some frequencies are shown for selected characteristic points.

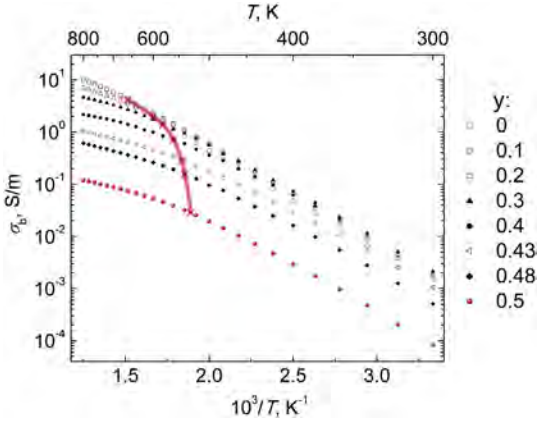

Fig. 3. Bulk conductivity Arrhenius plot for $Li_{0.5-y}Na_yLa_{0.5}Nb_2O_6$ compounds with different lithium concentration y. Thick red line approximately shows the change of activation energy. (For interpretation of the references to colour in this figure legend, the reader is referred to the web version of this article.)

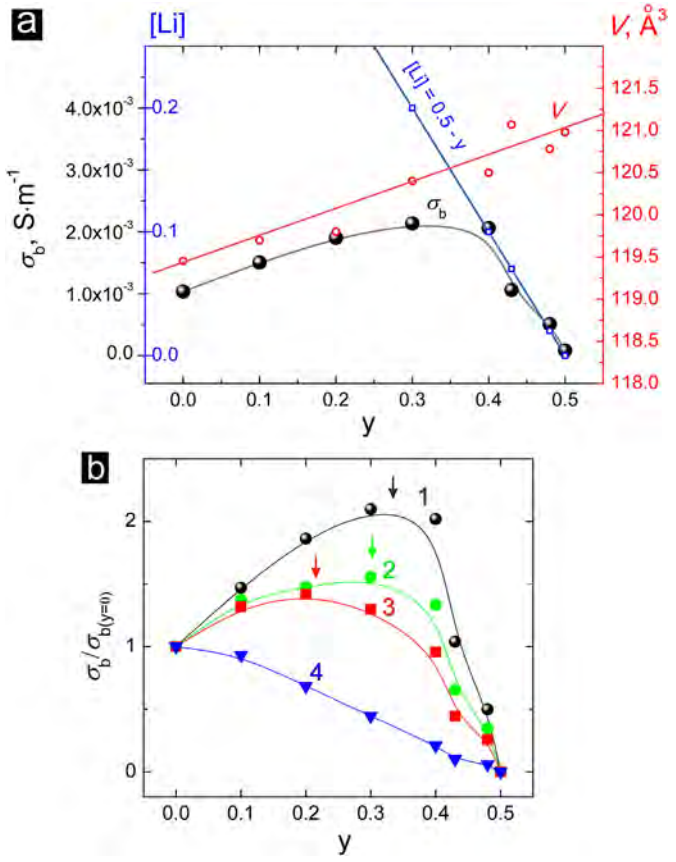

Fig. 4. Concentration dependences of $Li_{0.5-y}Na_yLa_{0.5}Nb_2O_6$ ceramics bulk conductivity at 300 K (a). Behaviour of the bulk conductivity can be explained by lattice volume increase and charge carrier concentration decrease with increasing stoichiometric factor y. (b) Dependence of normalized conductivity of $Li_{0.5-y}Na_yLa_{0.5}Nb_2O_6$ ceramics at different temperatures: 300 K (1), 400 K (2), 500 K (3), 800 K (4). Arrows show conductivity maxima, which shifts towards lower y values when temperature increases.

4. Discussion

In order to describe non-Arrhenius conductivity behaviour the theory proposed in [24] has been applied. The temperature dependent conductivity in the whole temperature range can be expressed as:

$$\sigma_b \cdot T = \frac{A_{\sigma T}\sqrt{T^2 - \left(\Delta\tilde{E}\Delta\tilde{Z}/R\right)^2}}{T} \exp\left(-\frac{\tilde{E}_0\tilde{Z}_0/R}{T - \Delta\tilde{E}\Delta\tilde{Z}/R}\right), \quad (4)$$

where $\tilde{E}$ is the bond energy between the mobile and the surrounding ion, $\tilde{Z}$ is the coordination number of the mobile ion, R is the gas constant, $\tilde{E}_0$ and $\tilde{Z}_0$ are the mean values of $\tilde{E}$ and $\tilde{Z}$, $\Delta\tilde{E}$ and $\Delta\tilde{Z}$ are their fluctuations and $A_{\sigma T} = g\nu(Ze)^2 l^2[Li^+]/Fk_B$, where g is geometrical factor, ν - oscillation frequency, l – jump distance and F – correlation factor. By appropriately choosing the parameters provided formula describes temperature dependence of conductivity of both the Arrhenius type and the Vogel–Fulcher–Tammann type. The parameters obtained from the experimental data fitting to formula (4) are presented in Table 3 and Fig. 5 shows the fitting result.

Authors [24] have shown, that for the system with low value of the fluctuation $\Delta\tilde{E}\Delta\tilde{Z}/R$, the model reduces to the Arrhenius-type behaviour. In fact, for the compound with y = 0 the best fitted value of $\Delta\tilde{E}\Delta\tilde{Z}/R$ was 0 and this shows the pure lithium compound to obey Arrhenius behaviour. It is also worth noting, that in the 2D conduction region ($0 < y \le 0.3$) the fitting parameters change significantly, while in the 3D conduction region the differences only for the preexponential factor are observed.

As it is shown in the formula (1), the conductivity is a product of charge, charge carrier concentration and mobility. As according to the chemical formula lithium concentration in $Li_{0.5-y}Na_yLa_{0.5}Nb_2O_6$ changes proportionally to (0.5 − y), dividing bulk conductivity by lithium amount in the formula we will get a quantity, which is proportional to the mobility of lithium ions. Composition dependences of $\sigma_b/(0.5 - y)$ are presented in Fig. 6.

At high temperature (i.e. 800 K) the mobility of lithium ions is the same for all compositions and the conductivity depends only on lithium concentration. Close to the room temperature the behaviour is different and lithium mobility significantly increases with increasing sodium fraction in the sample, so, as also discussed above, the conductivity at 300 K is determined by the mobility and lithium ion concentration.

At room temperature the maximum of conductivity as a function of sodium concentration in the system $Li_{0.5-y}Na_yLa_{0.5}Nb_2O_6$ can be explained by two competing effects, the one being the unit cell parameter change and the other – the change of mobile charge carriers. The increase of conductivity with increasing y (Fig. 4a)) is due to the increase of unit cell volume as can be seen from Tables 1 and 2. This, in accordance with [25], leads to the increase of bottleneck size and consequently to the conductivity increase and the activation energy decrease. With the further substitution of lithium by sodium (y > 0.4) the conductivity decreases because of significant decrease of charge carrier concentration, while charge carriers in this system are lithium-ions.

In order to find out the influence of the above mentioned factors on conductivity at elevated temperatures, the conductivity has been normalized to the value found for y = 0 and the normalized conductivity was studied as a function of lithium concentration (Fig. 4b)). As can be seen from the figure, with the temperature increase the maximum of conductivity becomes less pronounced and totally disappears at $T \ge 800$ K. However, the unit cell volume increases with temperature linearly (Tables 1 and 2). So we can conclude, that at 800 K the bottleneck size increases so much, that it stops limiting lithium mobility. Thus at high temperatures the change of unit cell parameters caused by lithium to sodium substitution does not affect the conductivity. The concentration dependencies of conductivity are affected only by lithium ion concentration, which is lowered when lithium is substituted by sodium. Consequently at 800 K lithium ion conductivity gradually lowers with the increase of y.

The potential barrier for lithium jumps is determined by the bottleneck size, which originates from structural features of the lattice and it

Table 3
Parameters of the model for non-Arrenius temperature dependence of ion conductivity of $Li_{0.5-y}Na_yLa_{0.5}Nb_2O_6$ determined in the present work following [24].

Chemical composition (y)	$\tilde{E}_0\tilde{Z}_0/R$ (K)	$\Delta\tilde{E}\Delta\tilde{Z}/R$ (K)	$\log A_{\sigma T}$ ($S \cdot K \cdot cm^{-1}$)
0	5885(96)	0	9.96(4)
0.1	5038(113)	8 (4)	9.60(5)
0.2	4204(139)	36(6)	9.09(6)
0.3	3501(120)	60(6)	8.58(6)
0.4	2830(78)	83(5)	7.90(4)
0.43	2814(71)	82(4)	7.55(4)
0.48	2832(73)	84(4)	7.34(4)
0.50	2791(88)	91(5)	6.63(5)

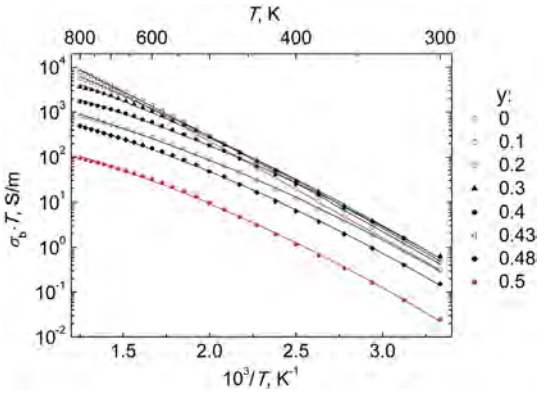

Fig. 5. Arrhenius plot of $Li_{0.5-y}Na_yLa_{0.5}Nb_2O_6$ ceramics conductivity. The fits to the Eq. (4) are shown as solid lines. Note that the conductivity is multiplied by temperature in this graph.

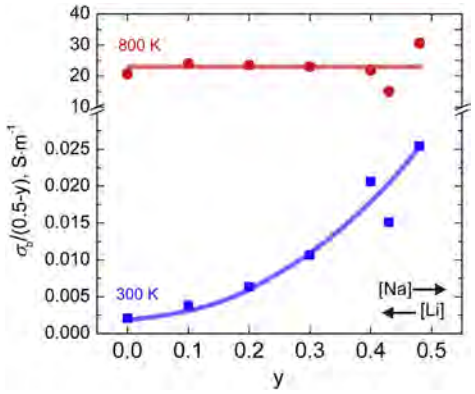

Fig. 6. Graph showing lithium mobility (see text) dependence on stoichiometric factor y at different temperatures. Arrows point out the increase of Na^+ and Li^+ concentrations in $Li_{0.5-y}Na_yLa_{0.5}Nb_2O_6$ ceramics, solid lines are guides for the eye.

increases with the expansion of unit cell when lithium is partially replaced by sodium. With the temperature increase the energy of thermal oscillations are supposed to increase significantly with regard to potential barrier for lithium-ion jumps. So the temperature dependences of conductivity at higher temperatures are determined by the lithium ion concentration rather than by the structural features of the lattice.

5. Conclusions

Lattice parameters of $Li_{0.5}La_{0.5}Nb_2O_6$ and $Na_{0.5}La_{0.5}Nb_2O_6$ change linearly with increase of temperature in the range from room temperature up to 900 °C. Grain conductivities of $Li_{0.5-y}Na_yLa_{0.5}Nb_2O_6$ ceramics have been studied from impedance spectra obtained by two-electrode method in the wide frequency range and temperatures up to 800 K. Non-Arrhenius temperature dependencies of grain conductivity were found except for the $Li_{0.5}La_{0.5}Nb_2O_6$ compound. Conductivity temperature dependencies were described by modified Vogel–Fulcher–Tammann equation. At lower temperatures a maximum of conductivity was found in the composition dependences. The character of the conductivity is affected by changes of lattice parameters and consequently the bottleneck size for Li^+-ion migration and also by charge carrier concentration. With the temperature increase this maximum shifts to lower y values and at high temperatures monotonous decrease of conductivity is observed when Li is replaced by Na. At 800 K lithium mobility was found to be independent on stoichiometric factor y in the system $Li_{0.5-y}Na_yLa_{0.5}Nb_2O_6$.

References

[1] A.D. Robertson, A.R. West, A.G. Ritchie, Solid State Ionics 104 (1997) 1.
[2] S. Megahed, B. Scrosati, J. Power Sources 51 (1994) 79.
[3] D.W. Murphy, P.A. Christian, Science 205 (1979) 651.
[4] P. Simon, Y. Gogotsi, Nat. Mater. 7 (2008) 845.
[5] S.M. Haile, Mater. Today 6 (2003) 24.
[6] A.G. Belous, G.N. Novitskaya, S.V. Polyanetskaya, Y.I. Gornikov, Izv. Akad. Nauk SSSR, Neorg. Mater. 23 (1987) 470.
[7] Y. Inaguma, L.Q. Chen, M. Itoh, T. Nakamura, T. Uchida, H. Ikuta, M. Wakihara, Solid State Commun. 86 (1993) 689.
[8] O. Bohnke, C. Bohnke, J.L. Fourquet, Solid State Ionics 91 (1996) 21.
[9] A. Rivera, C. León, J. Santamaría, A. Várez, A.G. Belous, O.I. V'yunov, J.A. Alonso, J. Sanz, Chem. Mater. 14 (2002) 5148.
[10] J. Sanz, A. Rivera, C. León, J. Santamaría, A. Várez, A.G. Belous, O. V'yunov, Mater. Res. Soc. Proc. 756 (2003) (EE2.31).
[11] C.P. Herrero, A. Varez, A. Rivera, J. Santamaria, C. Leon, A.G. Belous, O. V'yunov, J. Sanz, J. Phys. Chem. B 109 (2005) 3262.
[12] A.G. Belous, Ionics 4 (1998) 360.
[13] O. Bohnke, Solid State Ionics 179 (2008) 9.
[14] O. Bohnke, J. Emery, J.-L. Fourquet, Solid State Ionics 158 (2003) 119.
[15] O. Bohnke, J. Emery, A. Veron, J.L. Fourquet, J.Y. Buzare, P. Florian, D. Massiot, Solid State Ionics 109 (1998) 25.
[16] A. Belous, E. Pashkova, O. Gavrilenko, O. V'yunov, L. Kovalenko, J. Eur. Ceram. Soc. 24 (2004) 1301.
[17] A. Belous, E. Pashkova, O. Gavrilenko, O. V'yunov, L. Kovalenko, Int. J. Ion. 9 (2003) 21.
[18] A. Belous, O. Gavrilenko, O. Pashkova, O. Bohnké, C. Bohnké, Eur. J. Inorg. Chem. (2008) 4792.
[19] A.G. Belous, O.N. Gavrilenko, O.I. V'yunov, S.D. Kobilyanskaya, V.V. Trachevskii, Inorg. Mater. 47 (2011) 308.
[20] S.D. Kobylianska, O.I. V'yunov, A.G. Belous, O. Bohnke, Solid State Phenom. 200 (2013) 279.
[21] R. Jimenez, V. Dıez, J. Sanz, S.D. Kobylianska, O.I. V'yunov, A.G. Belous, RSC Adv. 5 (2015) 27912.
[22] A. Kezionis, S. Kazlauskas, D. Petrulionis, A.F. Orliukas, IEEE Trans. Microwave Theory Tech. 62 (2014) 2456.
[23] A. Kežionis, P. Butvilas, T. Šalkus, S. Kazlauskas, D. Petrulionis, T. Žukauskas, E. Kazakevičius, A.F. Orliukas, Rev. Sci. Instrum. 84 (2013) 013902.
[24] Y. Okada, M. Ikeda, M. Aniya, Solid State Ionics 281 (2015) 43.
[25] J.C. Bachman, S. Muy, A. Grimaud, H.H. Chang, N. Pour, S.F. Lux, O. Paschos, F. Maglia, S. Lupart, P. Lamp, L. Giordano, Y.S. Horn, Chem. Rev. 116 (2016) 140.